The University of Sydney

Department of Civil Engineering
Sydney NSW 2006
AUSTRALIA

http://www.civil.usyd.edu.au/

Centre for Advanced Structural Engineering

Displacement-based Formulations for Composite Beams with Longitudinal Slip and vertical Uplift

Research Report No R837

G Ranzi BE MScEng PhD
P Ansourian BSc BE PhD
F Gara BE MScEng PhD
G Leoni BE MScEng PhD
L Dezi BE MScEng PhD

January 2005

The University of Sydney

Department of Civil Engineering
Centre for Advanced Structural Engineering
http://www.civil.usyd.edu.au/

Displacement-based formulations for composite beams with longitudinal slip and vertical uplift

Research Report No R837

G. Ranzi, BE MScEng, PhD
P. Ansourian, BSc BE PhD
F. Gara, BE MScEng, PhD
G. Leoni, BE MScEng, PhD
L. Dezi, BE MScEng, PhD

Abstract:
This paper describes three novel displacement-based formulations for the analysis of composite beams with a flexible connection which is capable of deforming along the longitudinal axis of the member as well as vertically, i.e. transverse to the interface connection. For completeness, the analytical model which forms the basis of the proposed modelling technique is presented in both its weak and strong forms. The three novel finite element formulations are derived and tested using different structural systems; their nodal freedoms include the vertical and axial displacements as well as the rotations at each element end of both layers. Curvature locking problems are observed to occur for one of these elements and the origin of this behaviour is demonstrated analytically. Two applications are then proposed adopting a bi-linear constitutive relationship for the vertical interface connection to reflect the more realistic case in which, already in the linear-elastic range of the materials forming the cross-section and of the longitudinal interface connection, two vertical connection stiffnesses are required, i.e. one to model the event of separation between the layers and one when one bears against the other one.

Keywords:
Composite beams, Finite Element Method, Partial interaction, Slip, Uplift

Copyright Notice

Department of Civil Engineering, Research Report R837
Displacement-based formulations for composite beams with longitudinal slip and vertical uplift

G.Ranzi@civil.usyd.edu.au P.Ansourian@civil.usyd.edu.au

Published by:
Department of Civil Engineering
The University of Sydney
Sydney NSW 2006
AUSTRALIA

January 2005

This report and other Research Reports published by The Department of Civil Engineering are available on the Internet:

http://www.civil.usyd.edu.au

TABLE OF CONTENTS

1. INTRODUCTION p. 5

2. Theoretical Model p. 7
2.1 General p. 7
2.2 Displacement and strain fields p. 7
2.3 Material properties p. 9
2.4 Global equilibrium condition p. 9
2.5 Local equilibrium condition p. 11

3. Finite element formulation p. 12

4. Applications p. 13
4.1 Comparisons between the proposed finite elements p. 14
4.2 Curvature locking p. 15
4.2.1 High vertical and longitudinal interface connection stiffnesses p. 16
4.2.2 High longitudinal interface connection stiffness p. 16
4.3 Simply supported beam – 14dof finite element p. 17
4.4 Propped cantilever beam – 14dof finite element p. 18

5. CONCLUSIONS p. 18

APPENDIX 1 - REFERENCES p. 19

1 INTRODUCTION

In recent years great effort has been placed in the research and development of new materials and structural solutions. In some instances, such developments originate from an innovative combination of existing materials, such as composite materials. For this latter class of materials, different analytical formulations need to be utilised for an adequate modelling of their structural response depending upon the level of interaction present between the materials utilised. In the case the interaction as well as the stiffness of the connection are very high, the connection can be classified as rigid and the analysis of the non-homogeneous structural system can be carried out based on available modelling techniques [1,2]. On the other hand, in the case the deformability of the connection influences the structural behaviour, provisions for these effects need to be included in the theoretical model which reflects the partial interaction nature of these composites. In particular, longitudinal partial interaction highlights the ability of the connection to deform along the member axis, therefore leading to a longitudinal relative displacement between the two layers which is usually referred to in literature as slip, while vertical (transverse) partial interaction depicts the ability of the interface connection to deform vertically (transverse to the member axis), therefore producing a vertical relative displacement between the two layers which is referred to as uplift, which can be either positive or negative depending on whether vertical separation takes place between the two layers or one layer bears on the other one. The term 'transverse or vertical partial interaction' has been introduced in this paper to better highlight the deformations which take place at the interface between the two layers, while the term 'longitudinal partial interaction' is usually referred to in literature also as partial shear interaction [3].

Partial interaction problems are quite common in civil engineering applications; for example, in the cases of composite steel-concrete beams or of layered wood systems connected with nails or by means of other mechanical devices. It is worth noting that, even if this paper is mainly concerned with the behaviour of composite steel-concrete beams, the proposed formulation can be adopted for the analysis of generic composite systems which exhibit longitudinal and vertical partial interaction or to perform parametric studies to evaluate the influence of the partial interaction on the composite behaviour investigated.

The most cited work in the area of composite beams with longitudinal partial interaction is certainly the one by Newmark et al. [4], who highlighted the relevance of accounting for the deformability of the interface connection in a realistic modelling of the structural response of composite steel-concrete beams. Due to its wide spread, this formulation is usually simply referred to as Newmark's model. The main assumptions of this model require that no vertical separation occurs between the two layers and plane sections remain plane except for a discontinuity at the connection interface, i.e. longitudinal slip.
Since then, the longitudinal partial nature of composite beams has been studied extensively in the last decades in the linear-elastic range [5-10], in the nonlinear range [11-20], accounting for time effects [21-25] and including shear-lag effects [26]. For this purpose, various modelling techniques have been utilised, among the others the finite difference method, the finite element method and exact analytical solutions, while it is beyond the scope of this paper to provide an extensive list of references.

The first attempt to account also for the vertical partial interaction as well as the longitudinal shear one, therefore extending Newmark's model, was presented by

Adekola [27]. Experimentally the effects of both the vertical and the longitudinal partial interaction were observed and measured by Chapman and Balakrishnan [28] a few years earlier on steel-concrete composite beams. In Adekola's formulation [27], the governing system of differential equations was derived based on the equilibrium equations, in which the unknowns of the problem included the tensile (in the case of vertical separation) or compressive (in the case of vertical bearing) force per unit length and the shear flow at the interface (related to the longitudinal slip) as well as the moment distribution along the beam length. In this form, Adekola's model [27] is only applicable to the analysis of determinate structures as the moment distribution along the beam needs to be known a priori. In his solution procedure, the system of differential equations was solved by means of the finite difference method adopting a solution procedure proposed by Fox [29] for two-point boundary value problems involving differential equations of orders higher than two. Furthermore, he applied his modelling technique to the analysis of a simply supported beam subjected to a point load applied at the quarter point, and he adopted a constant value for the vertical connection stiffness for both events of separation of and bearing between the two layers. Robinson and Naraine [30] re-utilised Adekola's formulation [27] and, revisiting the problem of a simply supported beam subjected to a point load applied at the quarter point, solved it analytically. Similarly to Adekola [27], they adopted a constant value for the vertical connection stiffness and were able to solve the partial interaction problem as the bending distribution along the beam was known a priori. Around the same time, Aribert and Abdel Aziz [31] analysed the behaviour of determinate composite beams with a discrete distribution of shear connectors accounting for material nonlinearities by means of the transfer matrix method.

This paper proposes a novel analytical model for the analysis of composite beams with longitudinal and vertical partial interaction, which further extends previous work to handle also indeterminate beams. Based on the principle of virtual work the partial interaction problem is expressed in its weak form relying on a specified displacement field. For completeness, the full set of differential equations expressing the problem in its strong form is also presented.

Three novel finite elements are derived to carry out numerical applications, which possess 12dof, 14dof and 22dof respectively, and whose nodal freedoms include the vertical and axial displacements as well as the rotations of each layer at the ends of the element. The 12dof element relies on the lowest order shape functions required to model the partial interaction problem investigated. The remaining two elements represent different refinements of the basic 12dof element. Applications are presented to test the robustness of these proposed finite element formulations. Once the most economical (from a computational viewpoint) element capable of adequately model the partial interaction problem is identified, its ease of use is presented for the analysis of a determinate and an indeterminate structure, and for the purpose of these two applications, a bi-linear constitutive relationship is adopted to model the vertical interface connection for which two different stiffnesses are specified to better represent the realistic response of the structure already in the linear-elastic range of the materials forming the composite cross-section and of the longitudinal interface connection. One value of the vertical stiffness is used to describe the case when vertical separation occurs between the two layers, while the second value governs the behaviour when one layer is bearing against the other one. As the extent of the length of beam which undergoes vertical separation and along which bearing is taking place are not known a priori, an iterative procedure is utilised to determine the distribution of the two. Previous work did not address this

problem in their worked examples as a constant vertical connection stiffness was adopted throughout the beam length.

2. Theoretical Model

2.1 General

A prismatic composite beam formed by two layers, as shown in figure 1, is considered. In its undeformed state, the composite beam occupies the cylindrical region $V = A \times [0, L]$ generated by translating its cross-section A, with regular boundary ΩA, along a rectilinear axis which is orthogonal to the cross-section and is assumed to be parallel to the Z axis of the ortho-normal reference system $\{O;X,Y,Z\}$. For generality, the formulations are derived for a beam segment of length L and about an arbitrary coordinate system as shown in figure 1.

The composite cross-section is represented as $A = A_1 \cup A_2$, where A_1 and A_2 are the cross-sections of the top and bottom elements, which, for ease of reference, are referred to as elements 1 and 2 respectively, and it is assumed to be symmetric about the plane of bending with the coordinate plane YZ being taken as the plane of symmetry.

Without any loss of generality, the composite cross-section here represented is that of a typical steel concrete composite beam in which A_1 consists of the reinforced slab and it is further sub-divided into A_c and A_r, which represent the concrete component and the reinforcement respectively, i.e. $A_1 = A_c \cup A_r$, while A_2 represents the cross-section of the steel joist only and it is denoted as A_s.

2.2 Displacement and strain fields

The position of a generic material point P can be expressed in the undeformed state of the beam by the vector **r** as

$$\mathbf{r}(x, y, z) = x\mathbf{i} + y\mathbf{j} + z\mathbf{k} \qquad \forall (x, y) \in A = A_1 \cup A_2, \; z \in [0, L] \tag{1}$$

in which **i**,**j**,**k** represent the unit vectors parallel to the axes of the adopted ortho-normal reference system $\{O;X,Y,Z\}$. The composite action is provided by a connection which is assumed to be uniformly spread along a rectilinear line Λ at the interface between the two layers, whose domain consists of $(x,y) = (0,y_{rc})$ with $z \in [0, L]$, where y_{rc} is defined in figure 1. This interface connection allows relative displacements to occur in both longitudinal and vertical directions that, for clarity, will be referred to as longitudinal slip and vertical uplift.

The kinematic behaviour of the composite beam is expressed in terms of $u_1(z)$, $u_2(z)$, $v_1(z)$, and $v_2(z)$ which represent the axial displacements at the fibres located at y_1 and y_2 respectively, and the vertical deflections of layers 1 and 2 respectively (i.e. top and bottom layers), as shown in figure 2. This set of generalised displacements is collected in the vector **d** as

$$\mathbf{d}^{\mathrm{T}}(x, y, z) = [u_1(z) \;\; u_2(z) \;\; v_1(z) \;\; v_2(z)] \tag{2}$$

which will be simply referred to as u_1, u_2, v_1 and v_2 for ease of notation. For generality, the level of the reference axes y_1 and y_2 can be defined arbitrarily, which becomes particularly useful for structural applications, for example when accounting for nonlinear material properties.

The expressions for the rotations θ_1 (=$-v_1'$), θ_2 (=$-v_2'$) and curvatures κ_1 (=$-v_1''$), κ_2 (=$-v_2''$) along the beam can then be obtained by differentiating the relative deflections v_1 and v_2 with respect to the coordinate z along the beam length. The prime represents a derivative with respect to z. Under this assumption no torsional and out-of-plane flexural effects are considered. The two layers are assumed to obey the Euler-Bernoulli beam theory, while warping of the cross-section, i.e. shear-lag effects, is not considered.

The admissible displacement of a generic point in the composite beam can be defined, as illustrated in figure 2, by the following vectors:

$$\mathbf{d}_1(x,y,z) = v_1\mathbf{j} + \left[u_1 - (y-y_1)v_1'\right]\mathbf{k} \qquad \forall (x,y) \in A_1,\ z \in [0,L] \tag{3a}$$

$$\mathbf{d}_2(x,y,z) = v_2\mathbf{j} + \left[u_2 - (y-y_2)v_2'\right]\mathbf{k} \qquad \forall (x,y) \in A_2,\ z \in [0,L] \tag{3b}$$

in which $\mathbf{d_1}(x,y,z)$ and $\mathbf{d_2}(x,y,z)$ represent the displacements of the points in the domains of the top and bottom layers respectively, i.e. A_1 and A_2. For ease of notation, these have been collected in the vector $\mathbf{u}(x,y,z)$ which describes the displacement of the generic point P of the layer α (with $\alpha = 1,2$) as

$$\mathbf{u}(x,y,z) = \mathbf{d}_\alpha(x,y,z) \qquad \forall (x,y) \in A_\alpha,\ z \in [0,L] \tag{4}$$

The longitudinal slip and vertical uplift, which represent the kinematic discontinuities at the interface, are collected in the vector $\mathbf{s}$ as

$$\mathbf{s}(z) = \mathbf{d}_2(0,y_{rc},z) - \mathbf{d}_1(0,y_{rc},z) = s_y(z)\mathbf{j} + s_z(z)\mathbf{k} = (v_2 - v_1)\mathbf{j} + (u_2 - y_{r2}v_2' - u_1 + y_{r1}v_1')\mathbf{k} \tag{5}$$

in which s_z and s_y are the longitudinal slip and the vertical uplift respectively, $y_{r1} = y_{rc} - y_1$ and $y_{r2} = y_{rc} - y_2$, and y_{r1} and y_{r2} can assume both positive and negative values depending upon the reference system adopted as depicted in figure 1.

Based on the adopted displacement field, the relevant strain field can be obtained as

$$\varepsilon_x = \frac{\partial \mathbf{u}}{\partial x}\cdot\mathbf{i} = 0 \quad ; \quad \varepsilon_y = \frac{\partial \mathbf{u}}{\partial y}\cdot\mathbf{j} = 0 \tag{6a,b}$$

$$\varepsilon_z = \frac{\partial \mathbf{u}}{\partial z}\cdot\mathbf{k} = \varepsilon_{z_\alpha}(x,y,z) = u_\alpha' - (y-y_\alpha)v_\alpha'' \quad \forall (x,y) \in A_\alpha, z \in [0,L] \quad \text{with } \alpha = 1,2 \tag{6c}$$

$$\gamma_{xy} = \frac{\partial \mathbf{u}}{\partial y}\cdot\mathbf{i} + \frac{\partial \mathbf{u}}{\partial x}\cdot\mathbf{j} = 0 \ ; \ \gamma_{yz} = \frac{\partial \mathbf{u}}{\partial z}\cdot\mathbf{j} + \frac{\partial \mathbf{u}}{\partial y}\cdot\mathbf{k} = 0 \ ; \ \gamma_{xz} = \frac{\partial \mathbf{u}}{\partial z}\cdot\mathbf{i} + \frac{\partial \mathbf{u}}{\partial x}\cdot\mathbf{k} = 0 \tag{6d,e,f}$$

where ε_{z_1} and ε_{z_2} represent the non-vanishing strain components of the partial interaction problem.

2.3 Material properties

The constitutive models of the materials forming the composite cross-section obey Hooke's law in both tension and compression, and E_c, E_r and E_s are their elastic moduli (Young moduli) of the concrete, reinforcement and steel joist respectively. Hence,

$$\sigma_r(x,y,z) = E_r\left[u_1' - (y - y_1)v_1''\right] \tag{7a}$$
$$\sigma_s(x,y,z) = E_s\left[u_2' - (y - y_2)v_2''\right] \tag{7b}$$

where $\sigma_r(x,y,z)$ and $\sigma_s(x,y,z)$ represent stresses resisted by the reinforcement and steel joist at the composite cross-section. For generality, inelastic strains ε_{in} have been considered to be applied to the concrete component, for example due to thermal effects, which yields the following expression for the concrete stresses $\sigma_c(x,y,z)$

$$\sigma_c(x,y,z) = E_c\left[u_1' - \varepsilon_{in} - (y - y_1)v_1''\right] \tag{8}$$

The longitudinal and vertical partial interaction is modelled by means of a vertical and longitudinal connection uniformly spread at the interface between layers 1 and 2. The structural response of the longitudinal and vertical connections are assumed to be linear-elastic, and their constitutive relationships can be expressed as

$$q_z(z) = k_z s_z = k_z\left(u_2 - y_{r2}v_2' - u_1 + y_{r1}v_1'\right) \tag{9a}$$
$$q_y(z) = k_y s_y = k_y\left(v_2 - v_1\right) \tag{9b}$$

in which the connection stiffness k_z relates the longitudinal flow per unit length q_z to the corresponding longitudinal slip at the interface s_z, and k_y relates the force per unit length q_y to the uplift s_y.

2.4 Global equilibrium condition

The weak formulation of the partial interaction problem derived by means of the principle of virtual work can be expressed as

$$\int_L\int_A \sigma_z\hat{\varepsilon}_z \,\mathrm{d}a\,\mathrm{d}z + \int_L \left(q_z\hat{s}_z + q_y\hat{s}_y\right)\mathrm{d}z = \int_L\int_A \mathbf{b}\cdot\hat{\mathbf{u}}\,\mathrm{d}a\,\mathrm{d}z + \int_L\int_{\Omega A} \mathbf{p}\cdot\hat{\mathbf{u}}\,\mathrm{d}l\,\mathrm{d}z + \int_{A_{0,L}} \mathbf{p}\cdot\hat{\mathbf{u}}\,\mathrm{d}a \quad \forall\hat{\mathbf{u}} \tag{10}$$

in which ΩA represents the contour of the domain $A = A_1 \cup A_2$, σ_z represents those stresses which produce internal work, i.e. active stresses, q_z and q_y are the force per unit length which occur at the connection interface in the longitudinal and vertical directions respectively, and the third integral on the right hand-side of the equation represents the work carried out by the surface forces applied at the cross-section at the ends of the segment of beam considered. Virtual displacements and strains have been identified by means of a hat "^" placed above the variable considered.

In particular, the global balance condition expressed by equation (10) equates the work of the internal stresses to the work produced by the external actions for each kinematically admissible virtual displacement. The solution of the problem is then

sought in the spaces of the regular functions fulfilling the kinematic boundary conditions.

For generality, both quasi-static body and surface forces have been considered, and these have been referred to as **b** and **p** respectively.

The expression utilised in equation (10) to illustrate the weak formulation of the partial interaction problem can be re-arranged into the following compact form

$$\int_L \left[\left(\mathbf{K} D\ \mathbf{d} - \varepsilon_{in} \mathbf{f_{in}} \right) \cdot D\ \hat{\mathbf{d}} \right] \mathrm{d}z = \int_L \left(\mathbf{q} \cdot H \quad \hat{\mathbf{d}} \right) \mathrm{d}z + \left[\mathbf{Q} \cdot H \quad \hat{\mathbf{d}} \right]_{0,L} \qquad \forall \hat{\mathbf{d}} \tag{11}$$

and

$$\mathbf{q} = \begin{bmatrix} \int_{A_1} \mathbf{b} \cdot \mathbf{k}\, \mathrm{d}a + \int_{\Omega A_1} \mathbf{p} \cdot \mathbf{k}\, \mathrm{d}l \\ \int_{A_2} \mathbf{b} \cdot \mathbf{k}\, \mathrm{d}a + \int_{\Omega A_2} \mathbf{p} \cdot \mathbf{k} \mathrm{d}l \\ \int_{A_1} (y - y_1) \mathbf{b} \cdot \mathbf{k}\, \mathrm{d}a + \int_{\Omega A_1} (y - y_1) \mathbf{p} \cdot \mathbf{k}\, \mathrm{d}l \\ \int_{A_2} (y - y_2) \mathbf{b} \cdot \mathbf{k}\, \mathrm{d}a + \int_{\Omega A_2} (y - y_2) \mathbf{p} \cdot \mathbf{k}\, \mathrm{d}l \\ \int_{A_1} \mathbf{b} \cdot \mathbf{j}\, \mathrm{d}a + \int_{\Omega A_1} \mathbf{p} \cdot \mathbf{j}\, \mathrm{d}l \\ \int_{A_2} \mathbf{b} \cdot \mathbf{j}\, \mathrm{d}a + \int_{\Omega A_2} \mathbf{p} \cdot \mathbf{j}\, \mathrm{d}l \end{bmatrix} \quad ; \quad \mathbf{Q}_{0,L} = \begin{bmatrix} \overline{N}_1 \\ \overline{N}_2 \\ \overline{M}_1 \\ \overline{M}_2 \\ \overline{T}_1 \\ \overline{T}_2 \end{bmatrix}_{0,L} \tag{12a,b}$$

where **q**, $\mathbf{Q_0}$ and $\mathbf{Q_L}$ represent the vectors of actions applied along the beam and at the cross-sections at the ends of the beam segment considered, i.e. at $z = 0, L$. In particular, $\mathbf{f_{in}}$ is the vector related to the inelastic strain ε_{in} and **K** is the stiffness matrix defined as

$$\mathbf{f_{in}^T} = \begin{bmatrix} 0 & A_c E_c & 0 & 0 & 0 & 0 & B_c E_c & 0 & 0 & 0 \end{bmatrix} \tag{13a}$$

$$\mathbf{K} = \begin{bmatrix} k_z & 0 & -k_z & 0 & 0 & k_z y_{r1} & 0 & 0 & -k_z y_{r2} & 0 \\ 0 & A\tilde{E}_1 & 0 & 0 & 0 & 0 & B\tilde{E}_1 & 0 & 0 & 0 \\ -k_z & 0 & k_z & 0 & 0 & -k_z y_{r1} & 0 & 0 & k_z y_{r2} & 0 \\ 0 & 0 & 0 & A\tilde{E}_2 & 0 & 0 & 0 & 0 & 0 & B\tilde{E}_2 \\ 0 & 0 & 0 & 0 & k_y & 0 & 0 & -k_y & 0 & 0 \\ k_z y_{r1} & 0 & -k_z y_{r1} & 0 & 0 & k_z y_{r1}^2 & 0 & 0 & -k_z y_{r1} y_{r2} & 0 \\ 0 & B\tilde{E}_1 & 0 & 0 & 0 & 0 & I\tilde{E}_1 & 0 & 0 & 0 \\ 0 & 0 & 0 & 0 & -k_y & 0 & 0 & k_y & 0 & 0 \\ -k_z y_{r2} & 0 & k_z y_{r2} & 0 & 0 & -k_z y_{r1} y_{r2} & 0 & 0 & k_z y_{r2}^2 & 0 \\ 0 & 0 & 0 & B\tilde{E}_2 & 0 & 0 & 0 & 0 & 0 & I\tilde{E}_2 \end{bmatrix} \tag{13b}$$

in which the relevant cross-sectional properties are calculated as

$$A\tilde{E}_1 = \int_{A_c} E_c \, \mathrm{d}a + \int_{A_r} E_r \, \mathrm{d}a \quad ; \quad B\tilde{E}_1 = \int_{A_c} E_c (y - y_1) \, \mathrm{d}a + \int_{A_r} E_r (y - y_1) \, \mathrm{d}a \tag{14a,b}$$

$$I\tilde{E}_1 = \int_{A_c} E_c (y - y_1)^2 \, \mathrm{d}a + \int_{A_r} E_r (y - y_1)^2 \, \mathrm{d}a \tag{14c}$$

$$A\tilde{E}_2 = \int_{A_s} E_s \, \mathrm{d}a \quad ; \quad B\tilde{E}_2 = \int_{A_s} E_s (y - y_2) \, \mathrm{d}a \quad ; \quad I\tilde{E}_2 = \int_{A_s} E_s (y - y_2)^2 \, \mathrm{d}a \tag{14d,e,f}$$

and the formal differential operators D and H are determined as

$$D^{\mathrm{T}} = \begin{bmatrix} 1 & \partial & 0 & 0 & 0 & 0 & 0 & 0 & 0 & 0 \\ 0 & 0 & 1 & \partial & 0 & 0 & 0 & 0 & 0 & 0 \\ 0 & 0 & 0 & 0 & 1 & -\partial & -\partial^2 & 0 & 0 & 0 \\ 0 & 0 & 0 & 0 & 0 & 0 & 0 & 1 & -\partial & -\partial^2 \end{bmatrix} \tag{15a}$$

$$H^{\mathrm{T}} = \begin{bmatrix} 1 & 0 & 0 & 0 & 0 & 0 \\ 0 & 1 & 0 & 0 & 0 & 0 \\ 0 & 0 & -\partial & 0 & 1 & 0 \\ 0 & 0 & 0 & -\partial & 0 & 1 \end{bmatrix} \tag{15b}$$

2.5 Local equilibrium condition

The weak formulation proposed in equation (10) can be integrated by parts to yield the formulation of the partial interaction problem in its strong form, which can be expressed in compact form as

$$D^{*}(\mathbf{K} D\, \mathbf{d} - \varepsilon_{in}\mathbf{f}_{\mathbf{in}}) = H^{*}\mathbf{q} \tag{16}$$

and the relevant boundary conditions at the two end sections of the segment considered can be obtained as

$$\left[L\,(\mathbf{K} D\, \mathbf{d} - \varepsilon_{in}\mathbf{f}_{\mathbf{in}}) + P\,\mathbf{q} - \mathbf{Q}\right] \cdot H^{*}\,\hat{\mathbf{d}}\Big|_{0,L} = 0 \qquad \forall \hat{\mathbf{d}}_{0,L} \tag{17}$$

which express the kinematic conditions when $\hat{\mathbf{d}} = 0$ and the dual static conditions when $\hat{\mathbf{d}} \neq 0$, while D^{*}, H^{*}, L and P are operators defined as follows:

$$D^{*} = \begin{bmatrix} 1 & -\partial & 0 & 0 & 0 & 0 & 0 & 0 & 0 & 0 \\ 0 & 0 & 1 & -\partial & 0 & 0 & 0 & 0 & 0 & 0 \\ 0 & 0 & 0 & 0 & 1 & \partial & -\partial^2 & 0 & 0 & 0 \\ 0 & 0 & 0 & 0 & 0 & 0 & 0 & 1 & \partial & -\partial^2 \end{bmatrix} \tag{18a}$$

$$H^{*} = \begin{bmatrix} 1 & 0 & 0 & 0 & 0 & 0 \\ 0 & 1 & 0 & 0 & 0 & 0 \\ 0 & 0 & \partial & 0 & 1 & 0 \\ 0 & 0 & 0 & \partial & 0 & 1 \end{bmatrix} \tag{18b}$$

$$L = \begin{bmatrix} 0 & 1 & 0 & 0 & 0 & 0 & 0 & 0 & 0 & 0 \\ 0 & 0 & 0 & 1 & 0 & 0 & 0 & 0 & 0 & 0 \\ 0 & 0 & 0 & 0 & 0 & 0 & 1 & 0 & 0 & 0 \\ 0 & 0 & 0 & 0 & 0 & 0 & 0 & 0 & 0 & 1 \\ 0 & 0 & 0 & 0 & 0 & -1 & \partial & 0 & 0 & 0 \\ 0 & 0 & 0 & 0 & 0 & 0 & 0 & 0 & -1 & \partial \end{bmatrix} \tag{18c}$$

$$P = \begin{bmatrix} 0 & 0 & 0 & 0 & 0 & 0 \\ 0 & 0 & 0 & 0 & 0 & 0 \\ 0 & 0 & 0 & 0 & 0 & 0 \\ 0 & 0 & 0 & 0 & 0 & 0 \\ 0 & 0 & 1 & 0 & 0 & 0 \\ 0 & 0 & 0 & 1 & 0 & 0 \end{bmatrix} \tag{18d}$$

3. Finite element formulation

Three novel finite elements are proposed in this section, i.e. 12*dof*, 14*dof* and 22*dof* formulations, and their corresponding freedoms are depicted in figures 3.

The 12*dof* element utilizes the lowest order of polynomials which are capable of handling the proposed partial interaction problem, and these consist of a cubic and a linear function for the vertical and axial displacements of the two layers. The 14*dof* utilizes the same polynomial of the 12*dof* element for the deflection while specifying a parabolic function for the axial displacements. For this purpose, two additional internal nodes are inserted to provide a contribution of the same order from the vertical and axial displacements to the longitudinal slip. This latter condition is also satisfied by the 22*dof* element which possesses ten additional internal freedoms as shown in figure 3(c). The 22*dof* element enhances the order of both approximated fields to the fifth order for the deflections and to the fourth for the axial displacements of the two layers.
The unknown displacements for each of the element presented are approximated by a linear combination of interpolating shape functions according to

$$\mathbf{d} \cong \mathbf{N_e} \mathbf{d_e} \tag{19}$$

where $\mathbf{d_e}$ is the vector of the unknown nodal displacements which are outlined in figure 3 for the three elements considered, and $\mathbf{N_e}$ is the interpolation matrix collecting the relevant shape functions.

The proposed finite elements have been derived substituting equation (19) into the weak formulation of the partial interaction problem outlined in equation (11), which yields the following expression for an element

$$\begin{aligned} &\int_{L_e} \left[(D\ \mathbf{N_e})^T \mathbf{K} (D\mathbf{N_e}) \right] \mathrm{d}z\, \mathbf{d_e} \cdot \hat{\mathbf{d}}_\mathbf{e} = \\ &= \int_{L_e} \left[(D\ \mathbf{N_e})^T \mathbf{f_{in}} \right] \mathrm{d}z\, \varepsilon_{in} \cdot \hat{\mathbf{d}}_\mathbf{e} + \left\{ \int_{L_e} \left[(H\quad \mathbf{N_e})^T \mathbf{q} \right] \mathrm{d}z + \left[(H\quad \mathbf{N}_e)^T \mathbf{Q} \right]_{0,L_e} \right\} \cdot \hat{\mathbf{d}}_\mathbf{e} \qquad \forall \hat{\mathbf{d}}_\mathbf{e} \end{aligned} \tag{20}$$

This can be re-arranged at element level as

$$\mathbf{K_e d_e} = \varepsilon_{in}\mathbf{f_{e,in}} + \mathbf{q_e} \tag{21}$$

where $\mathbf{K_e}$ is the stiffness matrix of the element, $\mathbf{f_{e,in}}$ is the vector of nodal forces due to the inelastic strains, and $\mathbf{q_e}$ is the vector of the nodal external actions accounting for the forces distributed along the element and those concentrated at the end cross-sections of the element considered.
According to the principle of virtual work, the equilibrium condition for the whole structure can then be expressed by assembling the vectors and matrices defined for each element following the usual solution procedure of finite element formulations [1].

4. Applications

The robustness and performance of the proposed finite element formulations are tested in this section using, as case studies, a simply supported beam and a propped cantilever subjected to a point load applied to the bottom layer at mid-span. To better evaluate these formulations, different combinations of low and high connection stiffnesses have been considered, which are summarised in table 1 based on a dimensionless stiffness parameter αL proposed by Girhammar and Pan [10] for the case of longitudinal partial interaction only. For this purpose, a cross-section formed by a rectangular slab (2000 mm x 230 mm) with 1% reinforcement and a fabricated steel joist which has both flanges 250 mm $\times$ 16 mm and a web 660 mm $\times$ 10 mm has been used. The elastic modulus adopted for the steel reinforcement and joist is 210 000 MPa. A concrete strength f'_c of 32 MPa has been utilised, and the relevant material properties of the concrete have been calculated at 28 days following the design guidelines of [32]. Based on these results the most economical (from a computational viewpoint) element, while still robust in its modelling, is identified.

Using this preferred element, the cases of both the simply supported beam and the propped cantilever previously considered have been re-visited adopting a bi-linear constitutive relationship for the vertical interface connection as shown in figure 4, while still keeping the remaining constitutive models, i.e. concrete component, reinforcement, steel joist and longitudinal interface connection, in the linear-elastic range. For this purpose, the proposed bi-linear model is characterised by two stiffness parameters, i.e. $k_{y\gamma}$ (where $\gamma = s,b$ and these stand for 'separation' and 'bearing' respectively). This modification has been introduced to better describe the realistic structural response already at service loads when the materials forming the cross-section and the longitudinal connection are still in the linear-elastic range, in which case the bearing behaviour of the vertical connection is much stiffer than the response resisting the separation of the two layers, i.e. $k_{yb} >> k_{ys}$ where the bearing stiffness is several orders greater than the stiffness governing the separation between the two layers.

In the applications it has been assumed that the restraints provided by the pinned or roller supports of the simply supported beam are applied to the bottom element, while the top element, i.e. element 1, is supported by element 2 by means of the vertical connection. A similar condition has been specified for the propped cantilever

beam, for which the axial displacement and rotation have been prevented for both layers at the fixed support, while the vertical displacement has been restrained only for the bottom layer, and also in this case the top layer is supported by the bottom one. This has been carried out here to reflect a more realistic modelling; nevertheless, other support conditions can be easily implemented in the solution procedure.

4.1 Comparisons between the proposed finite elements

The results obtained using the 12*dof*, 14*dof* and 22*dof* finite elements have been compared for different variables describing the structural response adopting different combinations of low and high stiffnesses for the vertical and longitudinal interface connections as described in table 1 and, when worth highlighting, have been plotted in figures 5 to 12 for the cases of a simply supported beam and a propped cantilever subjected to a point load applied to the lower layer at mid-span. The comparisons have been carried out at a very coarse discretisation, i.e. 4 elements unless noted otherwise, to better illustrate the behaviour of these elements. The results have been non-dimensionalised against the peak values of the results obtained with an extremely fine discretisation, i.e. 100 elements, using the 22*dof* element.

At low connection stiffnesses, i.e. as for case A, all formulations seem to describe well the structural response for the simply supported beam and for the propped cantilever, except for the curvature of the top element, i.e. element 1, in which case both the 12*dof* and 14*dof* elements appear to produce some jumps at the element nodes due to the differences in values calculated for the curvature based on the elements located on the left and right sides of the nodes (figures 5 and 6). Nevertheless, for finer discretisations the 14*dof* and the 22*dof* elements yield accurate results.

Increasing the longitudinal connection stiffness, as for case B, the 22*dof* element seems to perform very well already for coarse discretisations as outlined in figures 7 and 8, while the 14*dof* formulation requires finer meshes to yield accurate results. Unfortunately, the 12*dof* element incurs in a curvature locking problem which forces the slopes of the curvatures of the top and bottom layers to be related to each other, and this is demonstrated algebraically in the next section. This phenomena affects also the longitudinal slip as highlighted in figure 9(a), where all formulations seem not to be able to detect the local variations of the longitudinal slip along the member at coarse discretisations, i.e. 4 elements, while adopting a finer mesh good accuracy can be achieved by the 14*dof* and 22*dof* elements as shown in figure 9(b).

Considering case C, which adopts a low longitudinal connection stiffness combined with a high vertical one, figure 10(a) highlights how all formulations do not capture the local variations of the vertical uplift along the member length at coarse discretisations. These results improve refining the mesh as outlined in figure 10(b). For the other variables describing the structural response, the proposed finite formulations perform well.

In the case of high stiffness values for both longitudinal and vertical connections (case D), the 14*dof* and 22*dof* elements perform well already at coarse discretisations as depicted in figures 11 and 12 for the curvatures of the top and bottom layers, while the 12*dof* element incurs in a curvature locking problem which

reduces the order of the utilised displacement field, and this is demonstrated algebraically in the next section.
Based on these comparisons, the use of the 12*dof* element is discouraged for the modelling of the partial interaction problem, while both 14*dof* and 22*dof* formulations seem to possess adequate robustness; the former one is preferred due to its computational savings it can lead to, even if at times finer discretisations than the 22*dof* element are required. Therefore, the remaining applications will be carried out using the 14*dof* element.

4.2 Curvature locking

Two curvature locking phenomena have been observed to occur when using the 12*dof* element in the previous applications, i.e. for case B (high longitudinal connection stiffness) and case D (high longitudinal and vertical connection stiffnesses). The origin of this behaviour is demonstrated algebraically in the following.

For clarity, the polynomial utilised for the axial and vertical displacements (for the 12*dof* element) are proposed below (with $\alpha = 1,2$ for the top and bottom layers respectively).

$$v_\alpha = \gamma_{\alpha 3}\xi^3 + \gamma_{\alpha 2}\xi^2 + \gamma_{\alpha 1}\xi + \gamma_{\alpha 0} \tag{22a}$$

$$u_\alpha = \bar{\gamma}_{\alpha 1}\xi + \bar{\gamma}_{\alpha 0} \tag{22b}$$

and

$$\gamma_{\alpha 3} = L_e\theta_{\alpha 0} + 2v_{\alpha 0} - 2v_{\alpha L} + L_e\theta_{\alpha L} \tag{23a}$$

$$\gamma_{\alpha 2} = 3v_{\alpha L} - 3v_{\alpha 0} - 2L_e\theta_{\alpha 0} - L_e\theta_{\alpha L} \tag{23b}$$

$$\gamma_{\alpha 1} = L_e\theta_{\alpha 0} \tag{23c}$$

$$\gamma_{\alpha 0} = v_{\alpha 0} \tag{23d}$$

$$\bar{\gamma}_{\alpha 1} = u_{\alpha L} - u_{\alpha 0} \tag{23e}$$

$$\bar{\gamma}_{\alpha 0} = u_{\alpha 0} \tag{23f}$$

$$\xi = \frac{z}{L_e} \tag{23g}$$

where L_e represents the length of the finite element considered, and $v_{\alpha 0}$, $v_{\alpha L}$, $\theta_{\alpha 0}$, $\theta_{\alpha L}$, $u_{\alpha 0}$, and $u_{\alpha L}$ are the nodal freedoms at the element ends, i.e. vertical displacement, rotation and axial displacement, at $z = 0, L$.

The vertical uplift and longitudinal slip can then be re-arranged based on the notation introduced in equations (23) as

$$s_z = u_2 - y_{r2}v_2' - u_1 + y_{r1}v_1' = \alpha_2\xi^2 + \alpha_1\xi + \alpha_0 \tag{24a}$$

$$s_y = v_2 - v_1 \tag{24b}$$

in which

$$\alpha_2 = -y_{r2}2\gamma_{23} + y_{r1}2\gamma_{13} \tag{25a}$$

$$\alpha_1 = -2y_{r2}\gamma_{22} + 2y_{r1}\gamma_{12} + \frac{\bar{\gamma}_{21} - \bar{\gamma}_{11}}{L_e} \tag{25b}$$

$$\alpha_0 = u_{20} + y_{r1}\theta_{10} - u_{10} - y_{r2}\theta_{20} \tag{25c}$$

4.2.1 High vertical and longitudinal interface connection stiffnesses

When both longitudinal and vertical interface stiffnesses tend to infinity, i.e. $k_y \to \infty$ and $k_z \to \infty$, both relative displacements, i.e. s_y and s_z, vanish due to the rigidity of the connection; this reflects the situation of case D. This kinematic requirement translates in the following conditions which relies on the notation presented in equation (24a):

$$\alpha_2 = \alpha_1 = \alpha_0 = 0 \tag{26}$$

Unfortunately, the conditions expressed by equation (26) produce a kinematic restraint on the displacement field of the vertical displacement which reduces its order by one degree, i.e. from a cubic polynomial down to a parabolic one.

Algebraically, this can be proven by noting that the limit $k_y \to \infty$ forces the vertical displacements and rotations of the two layers at each element ends to coincide and, therefore, the expressions for α_i (with $i = 1,2,3$) previously defined in equations (25) can be simplified as

$$\alpha_2 = 2(y_{r1} - y_{r2})(L_e\theta_0 + 2v_0 - 2v_L + L_e\theta_L) \tag{27a}$$

$$\alpha_1 = 2(y_{r1} - 2y_{r2})(3v_L - 3v_0 - 2L_e\theta_0 - L_e\theta_L) + \frac{\bar{\gamma}_{21} - \bar{\gamma}_{11}}{L_e} \tag{27b}$$

$$\alpha_0 = u_{20} - u_{10} + (y_{r1} - y_{r2})\theta_0 \tag{27c}$$

where v_0, θ_0, v_L, and θ_L represent the deflections and rotations at the element ends of both layers (which coincide for elements 1 and 2 when k_y tends to infinity), while the additional limit $k_z \to \infty$ requires also equation (26) to be satisfied. In particular, the condition of $\alpha_2 = 0$ produces the additional restraint of

$$\alpha_2 = \gamma_{13} = \gamma_{23} = L_e\theta_0 + 2v_0 - 2v_L + L_e\theta_L = 0 \tag{28}$$

which reduces the order of the deflection function defined in equation (22a) to

$$v_\alpha = \gamma_{\alpha 2}\xi^2 + \gamma_{\alpha 1}\xi + \gamma_{\alpha 0} \tag{29}$$

therefore providing a condition of curvature locking as the element would be able to produce only constant curvature along its length.

4.2.2 High longitudinal interface connection stiffness

A second type of curvature locking was observed to occur when the value of the longitudinal interface connection stiffness only tends to infinity (case B), i.e. $k_z \to \infty$. In this case, the slopes of the curvatures calculated for the top and bottom layers are dependent. This can be demonstrated algebraically by noting that for $k_z \to \infty$ the

longitudinal slip vanishes, and this can be achieved based on equation (24a) only if $\alpha_i = 0$ ($i = 1,2,3$). The condition of $\alpha_2 = 0$ produces a limitation on the variation of the first derivatives of the curvatures of the two layers as

$$y_{r2} 2\gamma_{23} = y_{r1} 2\gamma_{13} \tag{30}$$

This relationship between the first derivatives of the curvatures of the two layers can be expressed based on equation (22a) as ($\alpha = 1,2$)

$$v_\alpha''' = \frac{6\gamma_{\alpha 3}}{L_e^3} \tag{31}$$

and substituting equation (31) into equation (30) yields

$$v_2''' = \frac{y_{r1}}{y_{r2}} v_1''' \tag{32}$$

which reflects the fact that the slopes of the curvature, i.e. v_1" and v_2", are related to each other according to the ratio of y_{r1} and y_{r2}, previously defined as $y_{r1} = y_{rc} - y_1$ and $y_{r2} = y_{rc} - y_2$.

4.3 Simply supported beam – 14dof finite element

The analysis of a simply supported beam subjected to a point load applied at mid-span of the bottom layer is carried out in this section using the recommended 14*dof* element. For this purpose, a bi-linear model has been adopted for the vertical interface connection as shown in figure 4. Figure 13 outlines the results for this structural system. An iterative procedure has been implemented due to the presence of the bi-liner model for the vertical connection and, to better represents the results, the variables describing the structural response have been plotted for each iteration highlighting the results of the first one, the intermediate ones and the final one as well as the results obtained from Newmark's model [4]. These have been shown using non-dimensionalised values, while still allowing comparisons to be carried out between the different variables; for example, all displacements, i.e. vertical displacement, longitudinal slip and vertical uplift, have been plotted against the maximum deflection occurred in the bottom element, i.e. element 2, in order to highlight their relative magnitude. For the initial iteration the vertical connection stiffness specified along the full beam length is the one required in the case of vertical separation, while in successive iterations the vertical stiffness is modified to account for the results obtained at each iteration, till the analysis converges to its final solution.

For this application, the value of connection stiffness specified for the longitudinal interface connection and for the vertical one when separating yields a dimensionless stiffness parameter αL equal to 1, while the vertical stiffness specified when one layer is bearing against the other one produces a value of αL equal to 100. These values have been adopted here arbitrarily as the intent of these applications is to outline the ease of use of this novel modelling technique, while still keeping the connection stiffness in a relevant range of values.

It is interesting to note that the curvatures obtained by the proposed method and based on Newmark's model are very close for the bottom layer while in the case of the top layer these tend to have different values, as shown in figures 13(a) and 13(b); also, the top layer is not loaded directly from an external action but through the vertical connection. Despite the fact that the longitudinal slip, shown in figure 13(c) does not yield significant errors when compared to those based on the case of longitudinal partial interaction only, the magnitude of the vertical uplift is of the same order as the one of the longitudinal slip as depicted in figure 13(d). Therefore, in similar applications to the one considered, the proposed modelling technique should certainly be utilised to ensure an adequate modelling and behavioural representation of the interface connection. It is also interesting to note how the vertical force per unit length transmitted by the interface connection and the vertical uplift are affected by the subsequent iterations. Obviously, this observation is dependent upon the iteration procedure implemented. The different peaks outlined for the vertical force per unit length in figure 13(e) for the intermediate iterations highlight the situation in which the segments of the beam which are undergoing separation have been modelled using the vertical stiffness required for the bearing case, which is several orders of magnitude greater the former one. These peaks reduce between adjacent iterations till the final convergence is achieved.

4.4 Propped cantilever beam – 14dof finite element

Figure 14 illustrates the results obtained for the modelling of a propped cantilever beam subjected to a point load applied at mid-span of the bottom layer. Similarly to the case of the simply supported beam previously presented, an iterative procedure is adopted in the solution process to account for the bi-linear constitutive model of the vertical connection stiffness.

The results obtained for this application should be considered significant only from a qualitative viewpoint as it is likely for the concrete in the negative moment region to have undergone cracking. Nevertheless, this procedure is still very valuable, for example in evaluating how different combinations of cross-sectional properties and beam geometry affect the structural response.

The variations of the curvatures of the two layers, the longitudinal slip, the vertical uplift and the vertical force per unit length have been reported for each iteration, and where possible these results have been compared against those from Newmark's model.

Similar considerations to the ones presented for the simply supported case are applicable to this case, and in particular, the longitudinal slip and the vertical uplift are again of the same magnitude. Therefore, for situations similar to the one presented, the proposed formulation should be utilised to better investigate the influence of the vertical partial interaction.

5. CONCLUSIONS

This paper presented three novel displacement-based formulations for the analysis of composite beams with vertical and longitudinal partial interaction. These were derived based on a novel analytical model able to account for both the longitudinal

and vertical relative displacements between the two layers, which have been referred to as longitudinal slip and vertical uplift. Based on the principle of virtual work the partial interaction problem has been expressed in its weak form relying on a specified displacement field, and for completeness, the full set of differential equations expressing the problem in its strong form have also been presented.

The nodal freedoms of the three novel finite element formulations consist of the vertical and axial displacements and well as the rotations at each element end of both layers. In particular, the degrees of freedoms of the elements are 12*dof*, 14*dof* and 22*dof* respectively. These finite formulations have been tested for different combinations of the vertical and longitudinal connection stiffnesses to evaluate their robustness and the accuracy of their results. Based on these comparisons, the use of the 12*dof* element is discouraged for the modelling of the partial interaction problem as it is prone to two types of curvature locking problems which have been described and whose origins have been demonstrated analytically. Both 14*dof* and 22*dof* elements have been observed to perform well. Nevertheless, it has been observed that the 14*dof* finite element represents the most economical (from a computational viewpoint) element, as it is able to provide extremely accurate results already for relatively fine discretisations, and therefore its use is recommended for the modelling of composite beams with partial interaction.

Using the recommended 14*dof* element, a simply supported beam and a propped cantilever have been analysed using a bi-linear constitutive relationship for the vertical interface connection to reflect the more realistic case in which, already in the linear-elastic range of the materials forming the cross-section and of the longitudinal interface connection, two vertical connection stiffnesses need to be specified, i.e. one to model the event of separation between the two layers and one when one layer bears on the other one. An iterative procedure is utilised to account for this vertical bi-linear model as the extent of vertical connection which is engaging in a bearing mode or along which the two layers are separating is not known *a priori*. This proposed model forms a basis for investigating the influence of the vertical connection on the overall composite behaviour. It can be further extended to account for material nonlinearities and time effects.

APPENDIX 1 - REFERENCES

[1] Cook R, Malkus D, Plesha M, Witt R. *Concepts and applications of finite element analysis*. 4th edition, Wiley, 2001.

[2] Weaver W, Gere JM. *Matrix analysis of framed structures*. 3rd edition, Chapman & Hall, 1990.

[3] Oehlers DJ, Bradford MA. *Composite steel and concrete structural members: fundamental behaviour*. Pergamon Press, Oxford, 1995.

[4] Newmark NM, Siess CP, Viest IM. Tests and analysis of composite beams with incomplete interaction. *Proceedings of the Society of Experimental Stress Analysis* 1951; **9**(1): 75-92.

[5] Ranzi G, Bradford MA, Uy B. A direct stiffness analysis of a composite beam with partial interaction. *International Journal for Numerical Methods in Engineering* 2004; **61**: 657-672.

[6] Seracino R, Lee CT, Lim TC, Lim JY. Partial interaction stresses in continuous composite beams under serviceability loads. *Journal of Constructional Steel Research* 2004; **60**: 1525-1543.

[7] Wu YF, Oehlers DJ, Griffith MC. Partial-interaction analysis of composite beam/column members. *Mechanics of Structures and Machines* 2002; **30**(3): 309-332.
[8] Faella C, Martinelli E, Nigro E. Steel and concrete composite beams with flexible shear connection: "exact" analytical expression of the stiffness matrix and applications. *Computers and Structures* 2002; **80**: 1001-1009.
[9] Cosenza E, Mazzolani S. Linear-elastic analysis of composite beams with partial shear interaction. *Proceedings of the First Italian Workshop on Composite Structures*, University of Trento June 1993. (In Italian)
[10] Girhammar UA, Pan D. Dynamic analysis of composite members with interlayer slip. *International Journal of Solids and Structures* 1993; **30**(6): 797-823.
[11] Dall'Asta A, Zona A. Three-field mixed formulation for the non-linear analysis of composite beams with deformable shear connection. *Finite Elements in Analysis and Design* 2004; **40**: 425-448.
[12] Loh H, Uy B, Bradford MA. The effects of partial shear interaction in the hogging moment regions of composite beams: Part II – Analytical study. *Journal of Constructional Steel Research* 2004; **60**: 921-962.
[13] Faella C, Martinelli E, Nigro E. Steel connection nonlinearity and deflections of steel-concrete composite beams: a simplified approach. *Journal of Structural Engineering ASCE* 2003; **129**(1): 12-20.
[14] Ayoub A. A two-field mixed variational principle for partially connected composite beams. *Finite Elements in Analysis and Design* 2001; **37**: 929-959.
[15] Salari MR, Spacone E. Finite element formulations of one-dimensional elements with bond-slip. *Engineering Structures* 2001; **23**(7): 815-826.
[16] Ayoub A, Filippou FC. Mixed formulation of nonlinear steel-concrete composite beam element. *Journal of Structural Engineering ASCE* 2000 ; **126**(3): 371-381.
[17] Fabbrocino G, Manfredi G, Cosenza E. Analysis of continuous composite beams including partial interaction and bond. *Journal of Structural Engineering ASCE* 2000; **126**(11): 1288-1294.
[18] Gattesco N. Analytical modelling of nonlinear behaviour of composite beams with deformable connection. *Journal of Constructional Steel Research* 1999; **52**: 195-218.
[19] Nguyen NT, Oehlers DJ, Bradford MA. A rational model for the degree of interaction in composite beams with flexible shear connectors. *Mechanics of Structures and Machines* 1998 **26**(2): 175-194.
[20] Oehlers DJ, Sved G. Composite beams with limited-slip-capacity connectors. *Journal of Structural Engineering ASCE* 1995; **121**(6): 932-938.
[21] Virtuoso F, Vieira R. Time dependent behaviour of continuous composite beams with flexible connection. *Journal of Constructional Steel Research* 2004; **60**: 451-463.
[22] Fragiacomo M. Amadio C, Macorini L. Influence of viscous phenomena on steel-concrete composite beams with normal or high performance slab. *Steel and Composite Structures* 2002; **2**(2): 85-98.
[23] Kwak HG, Seo YL. Time-dependent behaviour of composite beams with flexible connectors. *Computer Methods in Applied Mechanics and Engineering* 2002; **191**: 3751-3772.
[24] Dezi L, Leoni G, Tarantino AM. Creep and shrinkage analysis of composite beams. *Progress in Structural Engineering and Materials* 1998; **1**(2): 170-177.
[25] Gilbert RI, Bradford MA. Time-dependent behavior of continuous composite beams at service loads. *Journal of Structural Engineering ASCE* 1995; **121**(2): 319-327.

[26] Dezi L, Gara F, Leoni G, Tarantino AM. Time dependent analysis of shear-lag effect in composite beams. *Journal of Engineering Mechanics* 2001; **127**(1): 71-79.
[27] Adekola AO. Partial interaction between elastically connected elements of a composite beam. *International Journal of Solids and Structures* 1968; **4**: 1125-1135.
[28] Chapman JC, Balakrishnan S. Experiments on composite beams. *Structural Engineer* 1964; **42**(11): 369-383.
[29] Fox L. *The numerical solution of two-point boundary problems in ordinary differential equations*. Oxford University Press, 1957.
[30] Robinson H, Naraine KS. Slip and uplift effects in composite beams. *Proceedings of the Engineering Foundation Conference on Composite Construction* (ASCE), 1988: 487-497.
[31] Aribert JM, Abdel Aziz K. Modelling of composite beams in ultimate state with vertical uplift. *Construction Métallique* 1985; **4**: 3-36. (In French)
[32] CEB-FIB (Comité Euro-International du Béton - Fédération International de la Précontrainte). *Model Code 1990: Design Code.* Thomas Telford, London, 1993.

	αL for vertical interface connection	αL for longitudinal interface connection
Case A	1	1
Case B	1	100
Case C	100	1
Case D	100	100

Table 1 – Rigidities adopted for the longitudinal and vertical interface connection utilised in the applications

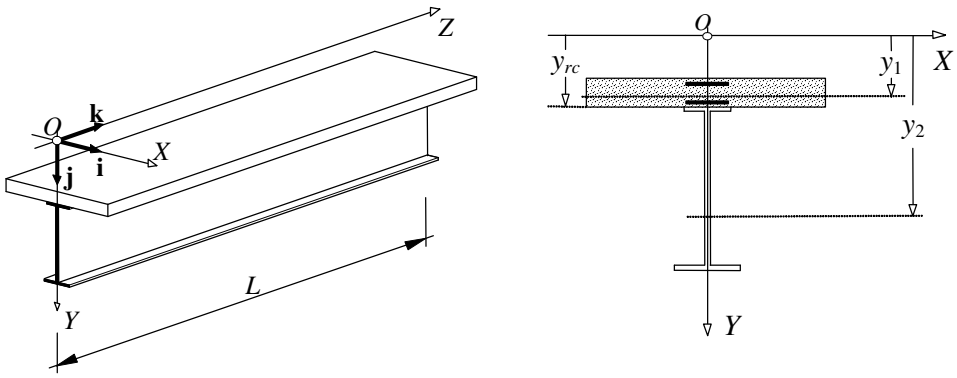

Fig. 1 – Typical composite beam and cross-section

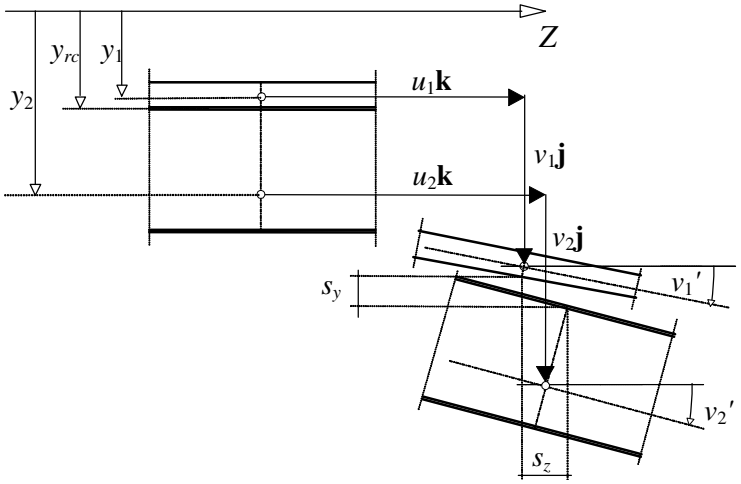

Fig. 2 – Displacement field

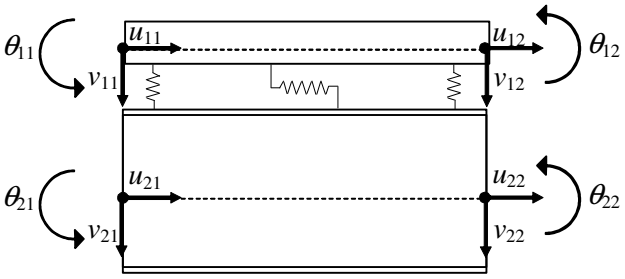

(a) 12*dof* finite element

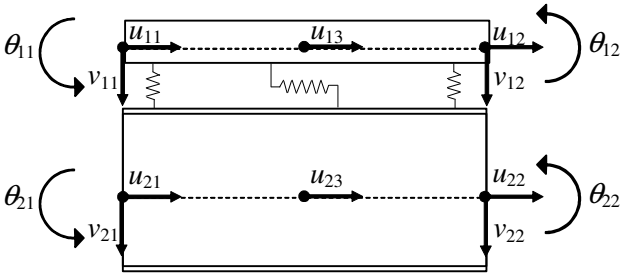

(b) 14*dof* finite element

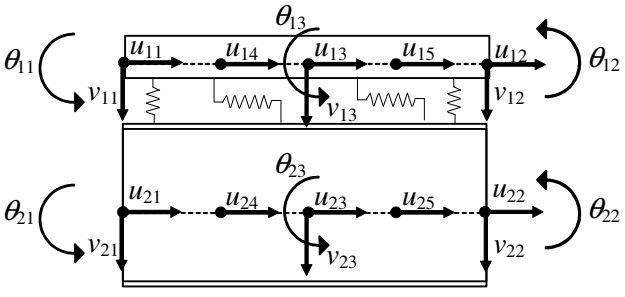

(c) 22*dof* finite element

Fig. 3 – Finite element formulations

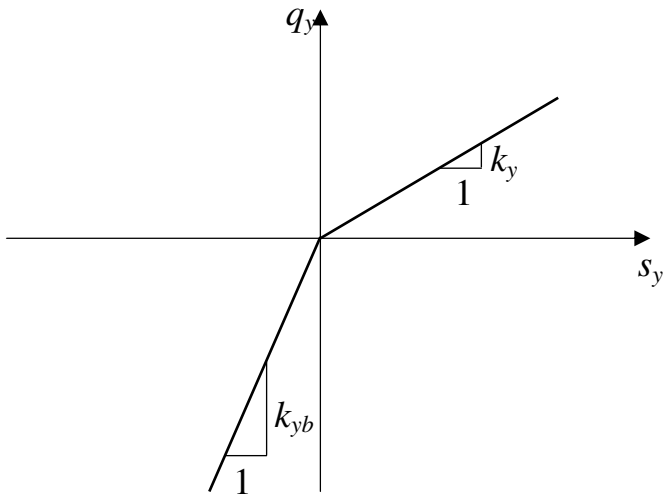

Fig. 4 – Bi-linear constitutive model for the vertical interface connection

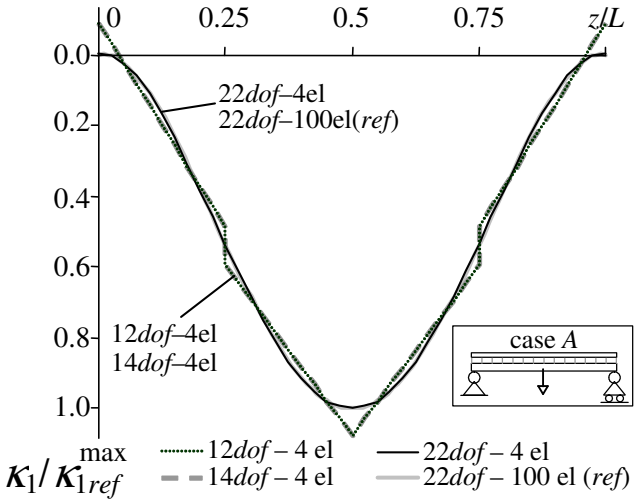

Fig. 5 – Curvature of element 1 for case A along a simply supported beam subjected to a point load applied at mid-span of the bottom element

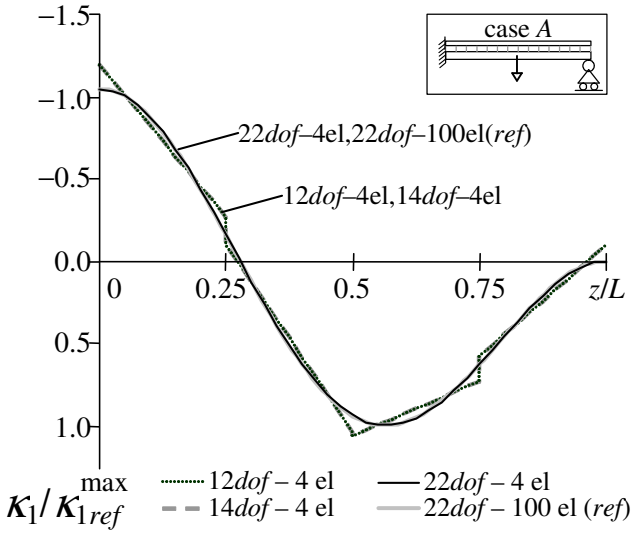

Fig. 6 – Curvature of element 1 for case A along a propped cantilever subjected to a point load applied at mid-span of the bottom element

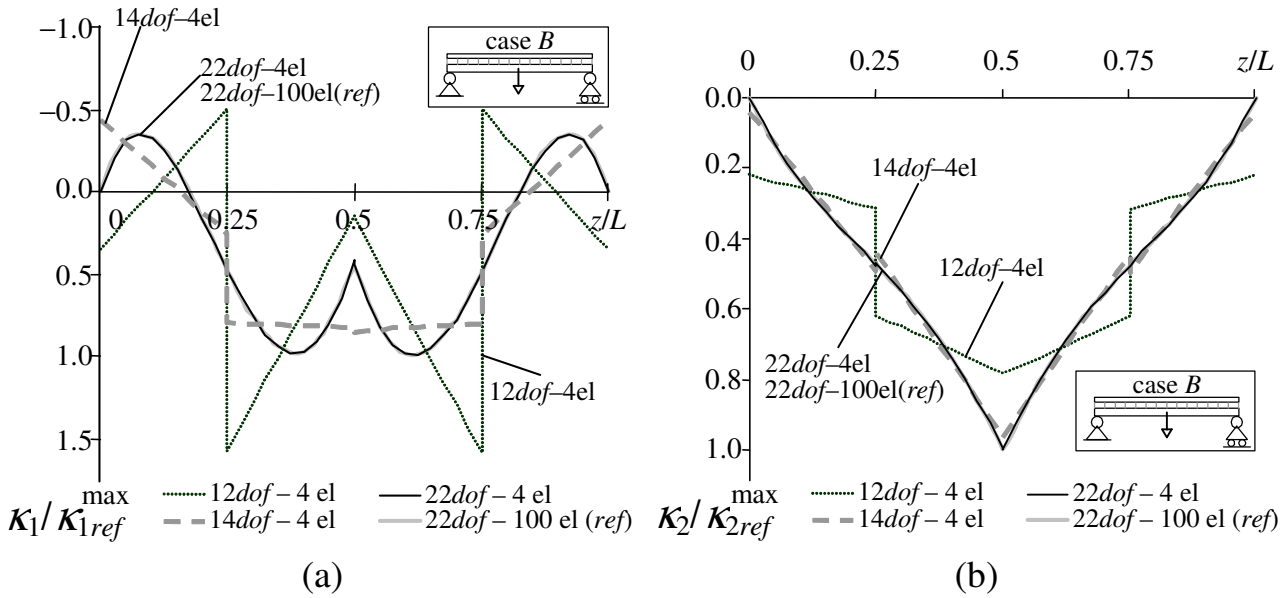

Fig. 7 – Curvature of elements 1 and 2 for case B along a simply supported beam subjected to a point load applied at mid-span of the bottom element

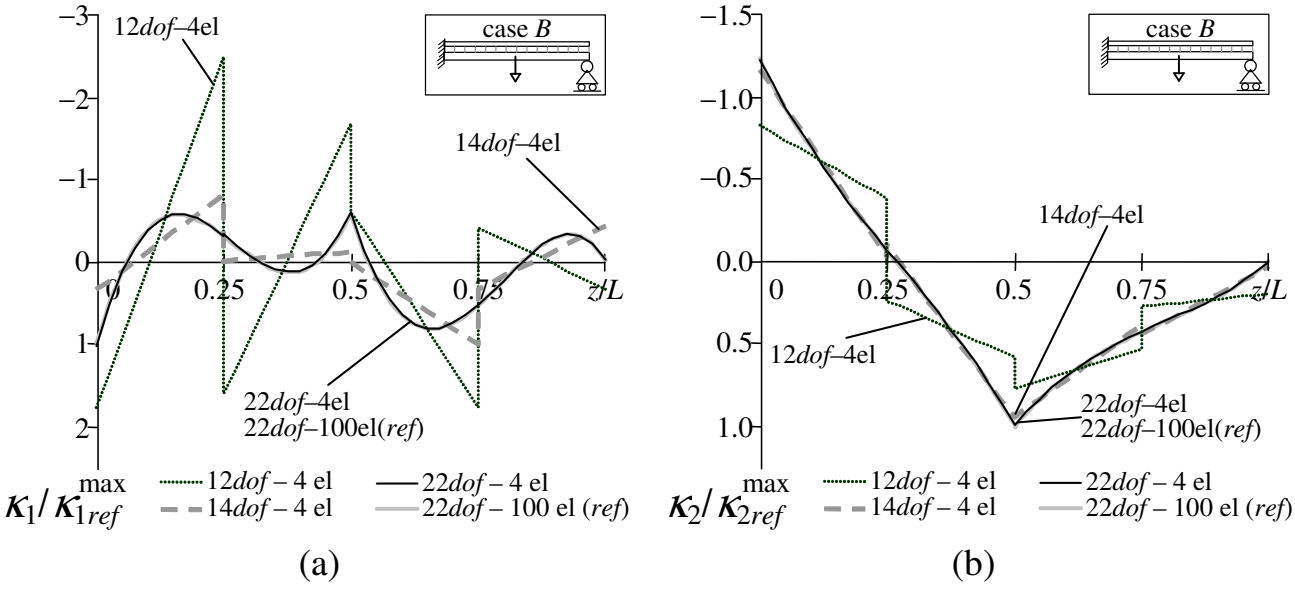

Fig. 8 – Curvature of elements 1 and 2 for case B along a propped cantilever subjected to a point load applied at mid-span of the bottom element

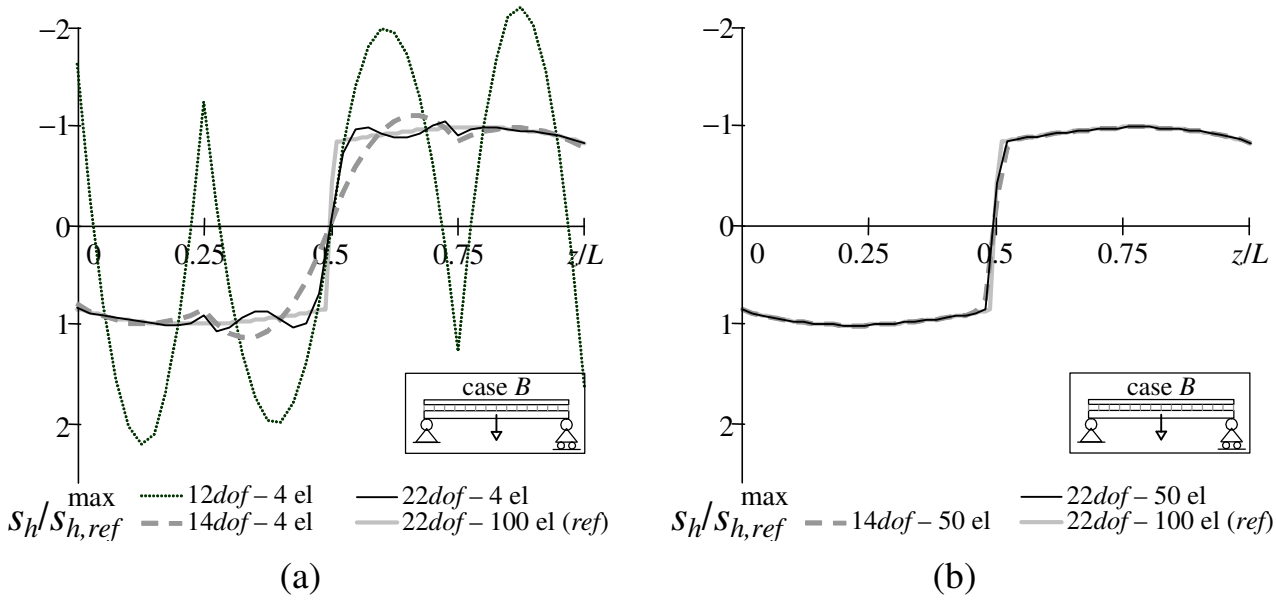

Fig. 9 – Longitudinal slip for case B along a simply supported beam subjected to a point load applied at mid-span of the bottom element

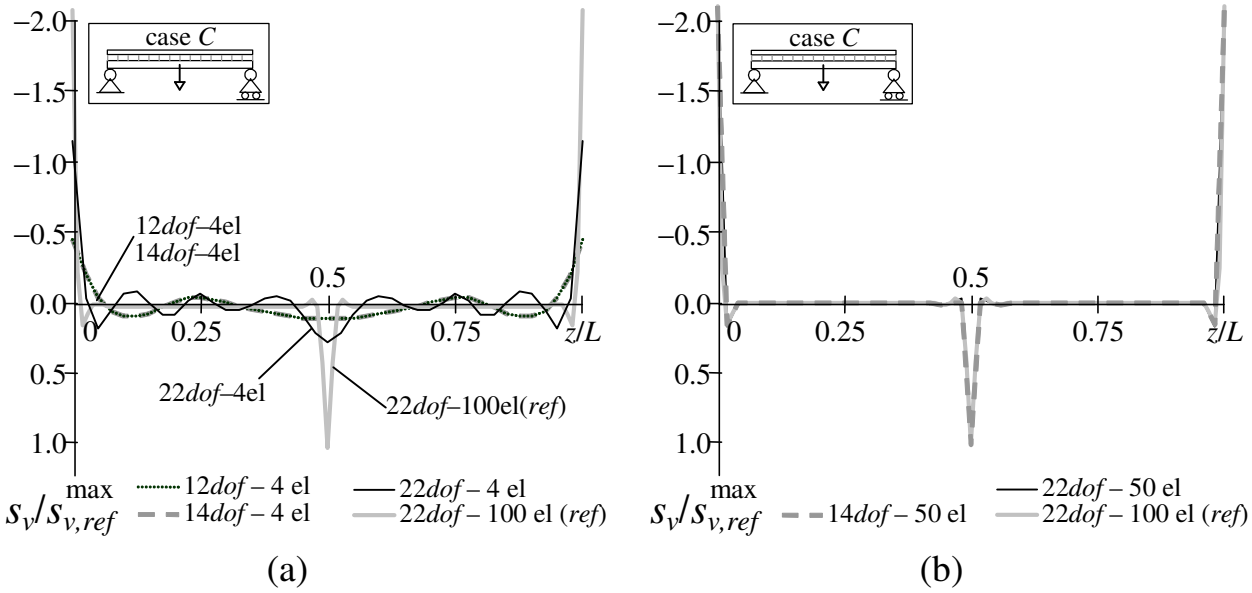

Fig. 10 – Vertical uplift for case C along a simply supported beam subjected to a point load applied at mid-span of the bottom element

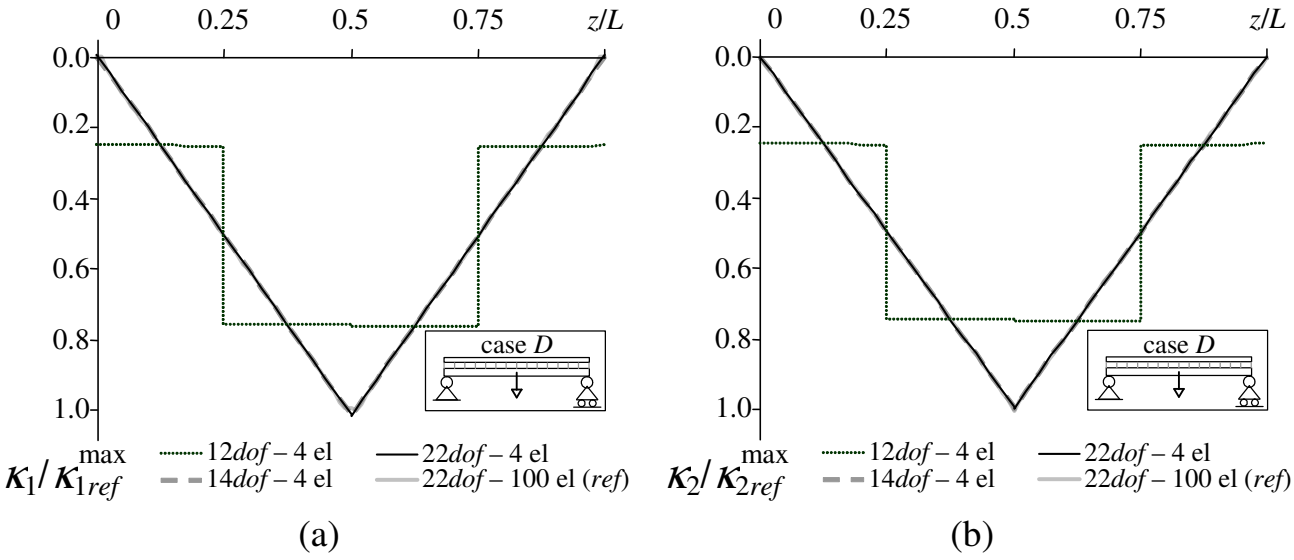

Fig. 11 – Curvature of elements 1 and 2 for case D along a simply supported beam subjected to a point load applied at mid-span of the bottom element

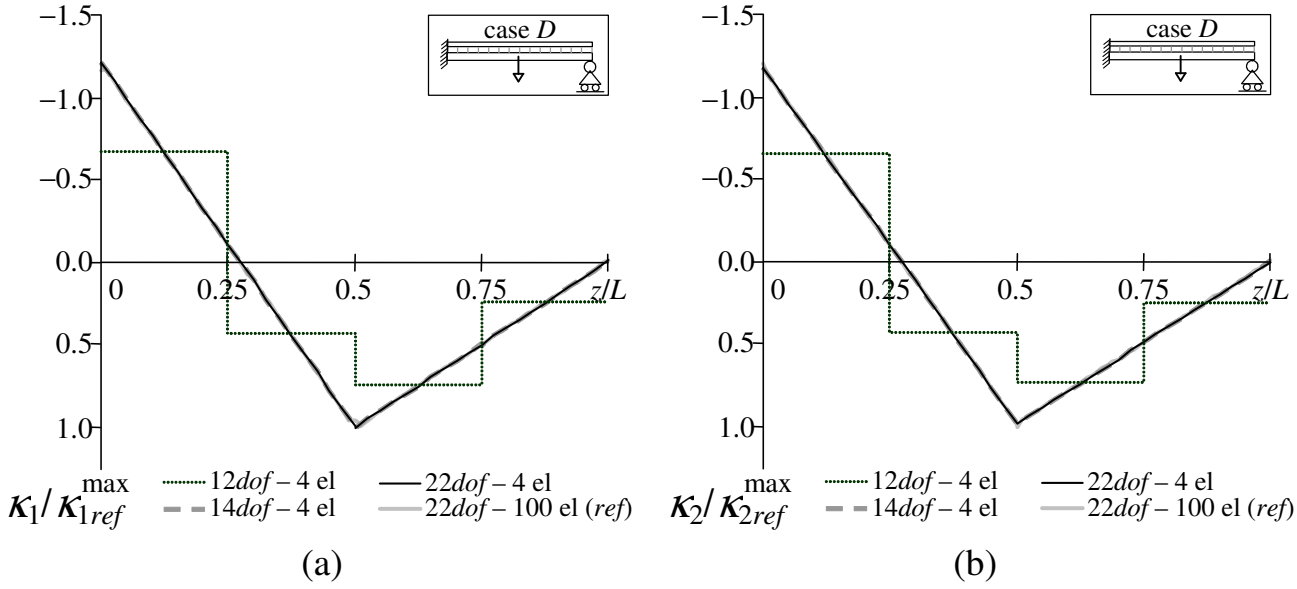

Fig. 12 – Curvature of elements 1 and 2 for case D along a propped cantilever subjected to a point load applied at mid-span of the bottom element

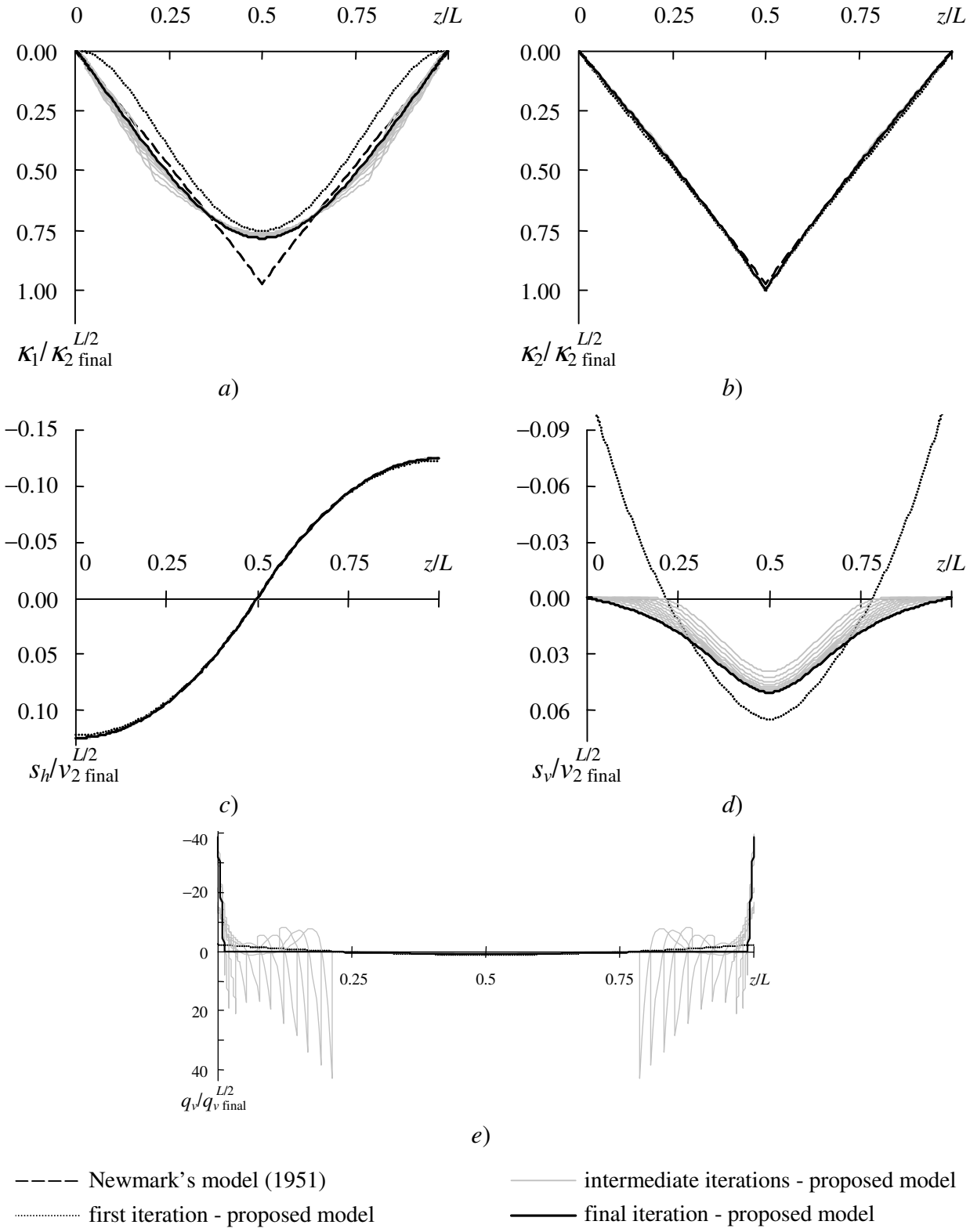

Fig. 13 – Simply supported beam subjected to a point load applied at mid-span of the bottom element - *a*) and *b*) Curvature of elements 1 and 2; *c*) and *d*) Longitudinal slip and vertical uplift; *e*) force per unit length resisted by the vertical connection

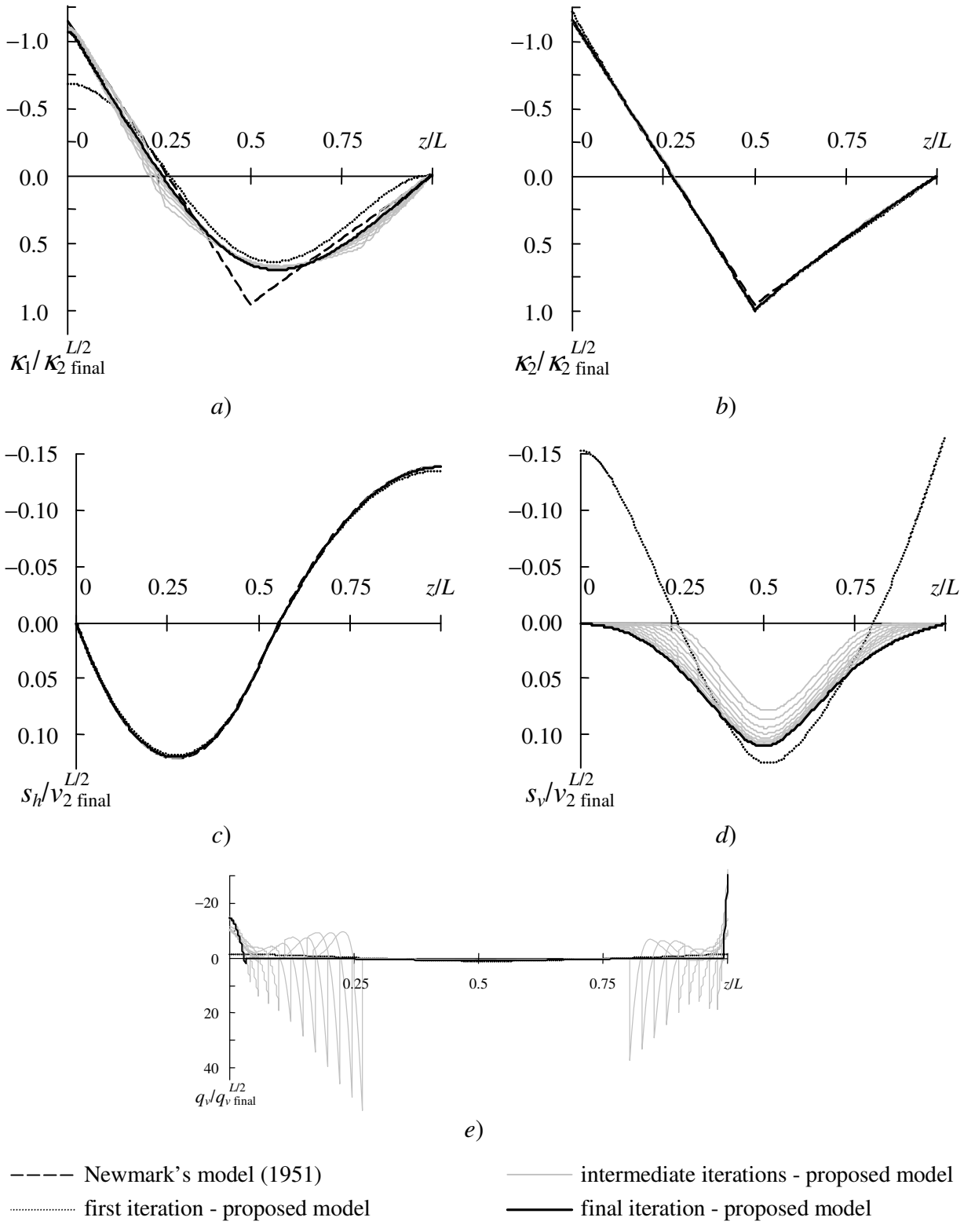

Fig. 14 – Propped cantilever beam subjected to a point load applied at mid-span of the bottom element - *a*) and *b*) Curvature of elements 1 and 2; *c*) and *d*) Longitudinal slip and vertical uplift; *e*) force per unit length resisted by the vertical connection